A Coarsening Method for Linear Peridynamics

S. A. Silling
Sandia National Laboratories
Albuquerque, New Mexico 87185-1322 USA
sasilli@sandia.gov

March 7, 2010

Abstract

A method is obtained for deriving peridynamic material models for a sequence of increasingly coarsened descriptions of a body. The starting point is a known detailed, small scale linearized state-based description. Each successively coarsened model excludes some of the material present in the previous model, and the length scale increases accordingly. This excluded material, while not present explicitly in the coarsened model, is nevertheless taken into account implicitly through its effect on the forces in the coarsened material. Numerical examples demonstrate that the method accurately reproduces the effective elastic properties of a composite as well as the effect of a small defect in a homogeneous medium.

1 Introduction

The problem of how to represent a complex microstructure with a reduced number of degrees of freedom is an important aspect of multiscale method development. For example, in molecular biology, one would like to represent a macromolecule by tracking a relatively small number of locations on the molecule, rather than simulating every atom in detail. In the mechanics of materials, the bulk properties of a continuum are determined by several length scales spanning many orders of magnitude. It would therfore be desirable have a rigorous and mathematically consistent technique for deriving the properties at each length scale from the one below it. For purposes of this paper, the process of deriving such a simplified model from a fully detailed model will be called *coarsening*.

The peridynamic theory of solid mechanics [10, 2] has been proposed as means of treating discontinuous media through a mathematical model that does not require a smooth distribution of mass or differentiability of the deformation. The starting point of the theory is that the internal forces acting on a material point are determined through interactions between the point and all others within a finite distance of it. The resulting mathematical model relies on integral equations that apply regardless of the smoothness of the mass distribution or of the deformation. The peridynamic model has a close resemblance to molecular dynamics in that it sums up forces on a point, or particle, acting across nonzero distances.

The linearized version of the peridynamic theory has been investigated in [11, 13, 4, 15, 6, 5, 14] and elsewhere. The equation of motion in the linearized theory is given by

$$\rho(\mathbf{x})\ddot{\mathbf{u}}(\mathbf{x},t) = \int_{\mathcal{N}_\mathbf{x}} \mathbf{C}(\mathbf{x},\mathbf{q})(\mathbf{u}(\mathbf{q},t) - \mathbf{u}(\mathbf{x},t))\, dV_\mathbf{q} + \mathbf{b}(\mathbf{x},t)$$

where ρ is the mass density, $\mathbf{u}$ is the displacement field, $\mathbf{b}$ is the body force density, $\mathbf{x}$ is position in the reference configuration, and t is time. $\mathcal{N}_\mathbf{x}$ is a neighborhood of $\mathbf{x}$ in which direct interactions with $\mathbf{x}$ are modeled.[1] $\mathbf{C}$ is a tensor-valued function called the *micromodulus* function. If the interaction between $\mathbf{x}$ and $\mathbf{q}$ is through a pair potential, then the form of $\mathbf{C}$ can be shown to be

$$\mathbf{C}(\mathbf{x},\mathbf{q}) = \lambda(\mathbf{x},\mathbf{q})(\mathbf{q}-\mathbf{x}) \otimes (\mathbf{q}-\mathbf{x}) + F_0(\mathbf{x},\mathbf{q})\mathbf{1} \tag{1}$$

where λ and F_0 are symmetric, scalar valued functions. Under this assumption of pair potentials, the bulk properties of a linear peridynamic material correspond to a Poisson ratio of 1/4. A significant generalization of the linear peridynamic theory was presented in [9], in which it is shown that any Poisson ratio, as well as various other material response, can be represented by a more general choice of $\mathbf{C}$ than (1). Alali and Lipton [1] considered the problem of homogenization within linear peridynamics. They obtained relations governing the displacement field within a periodic microstructure in the limit of small length scales.

The present paper addresses the problem of how to solve an equilibrium, linear peridynamic problem with a reduced level of geometrical detail. The method considers a succession of increasingly coarsened bodies derived from an original, detailed description. Each coarsening step involves the derivation of material properties from the previous step. The coarsened material

[1] As discussed in [9], the radius of $\mathcal{N}_\mathbf{x}$ is in general 2δ, where δ is the *horizon*. The horizon is the length scale of the constitutive model from which $\mathbf{C}$ is derived through linearization.

properties are determined so that the effect of the excluded material is implicitly included in the internal forces. In other words, deformation of the more detailed material affects the forces between the points in the coarsened model, even though it no longer appears explicitly. It is shown that by this procedure, the forces between points in the coarsened model agree with those that would be computed in the fully detailed model, but with much less computational effort. The process of coarsening can be repeated many times, until the model has sufficiently few degrees of freedom that an economical simulation can be performed.

The problem of coarsening a geometry is different from, but related to, mesh adaptivity, which was discussed in [3]. In mesh adaptivity, a given numerical model is refined where additional resolution is needed. In coarsening, the detailed geometry of a body is replaced by a succession of different geometries, with different properties, in such a way as to give essentially the same result as in the original detailed problem.

In the remainder of this paper, the theoretical development for the coarsening method is given. A discretized form of the coarsening method is presented, with example problems. The examples illustrate that after multiple coarsening steps, the method continues to reproduce the bulk properties of a one-dimensional composite material with a periodic microstructure. It is also demonstrated that the coarsening method, when applied in the vicinity of a material defect, continues to reproduce the essential features of the defect in a boundary value problem.

2 Coarsening a detailed model

Consider a linear elastic peridynamic body $\mathcal{B}^0$, and let $\mathcal{A}^0$ be the set of admissible displacement fields on $\mathcal{B}^0$. Let $\mathbf{C}^0 : \mathcal{B}^0 \times \mathcal{B}^0 \to \mathcal{L}$ be the micromodulus tensor field associated with the material, where $\mathcal{L}$ is the set of all second order tensors. Suppose there is a positive number r^0 representing the maximum interaction distance for points in $\mathcal{B}^0$:

$$|\mathbf{q} - \mathbf{x}| > r^0 \quad \Longrightarrow \quad \mathbf{C}^0(\mathbf{x}, \mathbf{q}) = \mathbf{0} \qquad \forall \mathbf{q}, \mathbf{x} \in \mathcal{B}^0.$$

Let $\mathcal{B}^1 \subset \mathcal{B}^0$, and let $\mathcal{A}^1$ be the set of admissible displacement fields on $\mathcal{B}^1$. $\mathcal{B}^0$ and $\mathcal{B}^1$ will be called the *level 0 body* and the *level 1 body* respectively (Figure 1). Our objective is to express the internal forces on $\mathcal{B}^1$ purely in terms of its own displacements, while taking into account forces that points in $\mathcal{B}^0 - \mathcal{B}^1$ exert on points in $\mathcal{B}^1$ due to their own displacements.

To do this, choose an arbitrary point $\mathbf{x} \in \mathcal{B}^1$. Let r^1 be a positive number, and let $\mathcal{N}^1_{\mathbf{x}}$ be the closed neighborhood of $\mathbf{x}$ in $\mathcal{B}^0$ with radius r^1 (Figure 2):

$$\mathcal{N}^1_{\mathbf{x}} = \big\{ \mathbf{q} \in \mathcal{B}^0 \;\big|\; |\mathbf{q} - \mathbf{x}| \leq r^1 \big\}.$$

Let $\mathcal{R}^1_{\mathbf{x}} = \mathcal{N}^1_{\mathbf{x}} \cap \mathcal{B}^1$. Suppose $\mathbf{u}^1 \in \mathcal{A}^1$ is given, and let $\mathbf{u}^0 \in \mathcal{A}^0$ satisfy the *compatibility* condition

$$\mathbf{u}^0(\mathbf{p}) = \mathbf{u}^1(\mathbf{p}) \qquad \forall \mathbf{p} \in \mathcal{R}^1_{\mathbf{x}}. \tag{2}$$

Outside of $\mathcal{R}^1_{\mathbf{x}}$, assume that $\mathbf{u}^0$ satisfies the equilibrium equation, neglecting interactions between $\mathcal{N}^1_{\mathbf{x}}$ and its exterior:

$$\mathbf{L}^0(\mathbf{z}) + \mathbf{b}(\mathbf{z}) = \mathbf{0} \qquad \forall \mathbf{z} \in \mathcal{N}^1_{\mathbf{x}} - \mathcal{R}^1_{\mathbf{x}} \tag{3}$$

where

$$\mathbf{L}^0(\mathbf{z}) = \int_{\mathcal{N}^1_{\mathbf{x}}} \mathbf{C}^0(\mathbf{z}, \mathbf{p})(\mathbf{u}^0(\mathbf{p}) - \mathbf{u}^0(\mathbf{z}))\, dV_{\mathbf{p}} \qquad \forall \mathbf{z} \in \mathcal{N}^1_{\mathbf{x}}. \tag{4}$$

Also assume that there is no body force density applied outside of $\mathcal{R}^1$:

$$\mathbf{b}(\mathbf{z}) = \mathbf{0} \qquad \forall \mathbf{z} \in \mathcal{N}^1_{\mathbf{x}} - \mathcal{R}^1_{\mathbf{x}}. \tag{5}$$

Further assume that for a given $\mathbf{u}^1$ field, (2) and (3) have a unique solution $\mathbf{u}^0$ on $\mathcal{N}^1_{\mathbf{x}}$, and let $\mathbf{S}^{0,1}_{\mathbf{x}}$ be the resolvent kernel that generates this solution:

$$\mathbf{u}^0(\mathbf{p}) = \int_{\mathcal{R}^1_{\mathbf{x}}} \mathbf{S}^{0,1}_{\mathbf{x}}(\mathbf{p}, \mathbf{q})\mathbf{u}^1(\mathbf{q})\, dV_{\mathbf{q}} \qquad \forall \mathbf{p} \in \mathcal{N}^1_{\mathbf{x}}. \tag{6}$$

From (2) and (6), we infer that

$$\mathbf{S}^{0,1}_{\mathbf{x}}(\mathbf{p}, \mathbf{q}) = \mathbf{1}\Delta(\mathbf{p} - \mathbf{q}) \qquad \forall \mathbf{p} \in \mathcal{R}^1_{\mathbf{x}},\ \forall \mathbf{q} \in \mathcal{N}^1_{\mathbf{x}} \tag{7}$$

where $\mathbf{1}$ is the identity tensor and Δ is the three dimensional Dirac delta function. For the special case of $\mathbf{u}^1$ representing a rigid translation of $\mathcal{R}^1$ through an arbitrary displacement vector, say $\bar{\mathbf{u}}$, then all the points in $\mathcal{N}^1_{\mathbf{x}} - \mathcal{R}^1_{\mathbf{x}}$ must also translate by the same vector. Therefore, from (6),

$$\bar{\mathbf{u}} = \left[\int_{\mathcal{R}^1_{\mathbf{x}}} \mathbf{S}^{0,1}_{\mathbf{x}}(\mathbf{p}, \mathbf{q})\, dV_{\mathbf{q}}\right] \bar{\mathbf{u}} \qquad \forall \text{ vectors } \bar{\mathbf{u}},\ \forall \mathbf{p} \in \mathcal{N}^1_{\mathbf{x}},$$

hence the following identity is obtained:

$$\int_{\mathcal{R}^1_{\mathbf{x}}} \mathbf{S}^{0,1}_{\mathbf{x}}(\mathbf{p}, \mathbf{q})\, dV_{\mathbf{q}} = \mathbf{1} \qquad \forall \mathbf{p} \in \mathcal{N}^1_{\mathbf{x}}. \tag{8}$$

Subtracting $\mathbf{u}^0(\mathbf{z})$ from both sides of (6), and using (8),

$$\mathbf{u}^0(\mathbf{p}) - \mathbf{u}^0(\mathbf{z}) = \int_{\mathcal{R}^1_{\mathbf{x}}} \mathbf{S}^{0,1}_{\mathbf{x}}(\mathbf{p}, \mathbf{q})(\mathbf{u}^1(\mathbf{q}) - \mathbf{u}^1(\mathbf{z}))\, dV_{\mathbf{q}} \qquad \forall \mathbf{p}, \mathbf{z} \in \mathcal{N}^1_{\mathbf{x}}.$$

Using this result in (4),

$$\mathbf{L}^0(\mathbf{z}) = \int_{\mathcal{N}_{\mathbf{x}}^1} \mathbf{C}^0(\mathbf{z},\mathbf{p}) \left[\int_{\mathcal{R}_{\mathbf{x}}^1} \mathbf{S}_{\mathbf{x}}^{0,1}(\mathbf{p},\mathbf{q})(\mathbf{u}^1(\mathbf{q}) - \mathbf{u}^1(\mathbf{z}))\, dV_{\mathbf{q}} \right] dV_{\mathbf{p}} \qquad \forall \mathbf{z} \in \mathcal{N}_{\mathbf{x}}^1.$$

Reversing the order of integration and rearranging,

$$\mathbf{L}^0(\mathbf{z}) = \int_{\mathcal{R}_{\mathbf{x}}^1} \left[\int_{\mathcal{N}_{\mathbf{x}}^1} \mathbf{C}^0(\mathbf{z},\mathbf{p}) \mathbf{S}_{\mathbf{x}}^{0,1}(\mathbf{p},\mathbf{q})\, dV_{\mathbf{p}} \right] (\mathbf{u}^1(\mathbf{q}) - \mathbf{u}^1(\mathbf{z}))\, dV_{\mathbf{q}} \qquad \forall \mathbf{z} \in \mathcal{N}_{\mathbf{x}}^1.$$

Recalling that $\mathbf{x}$ is an arbitrary point in $\mathcal{B}^1$, denote the force density at any such choice of $\mathbf{x}$ by

$$\mathbf{L}^1(\mathbf{x}) = \mathbf{L}^0(\mathbf{x}) \qquad \forall \mathbf{x} \in \mathcal{B}^1. \tag{9}$$

From this and the previous equation,

$$\mathbf{L}^1(\mathbf{x}) = \int_{\mathcal{R}_{\mathbf{x}}^1} \mathbf{C}^1(\mathbf{x},\mathbf{q})(\mathbf{u}^1(\mathbf{q}) - \mathbf{u}^1(\mathbf{x}))\, dV_{\mathbf{q}} \qquad \forall \mathbf{x} \in \mathcal{B}^1 \tag{10}$$

where $\mathbf{C}^1 : \mathcal{B}^1 \times \mathcal{B}^1$ is defined by

$$\mathbf{C}^1(\mathbf{x},\mathbf{q}) = \int_{\mathcal{N}_{\mathbf{x}}^1} \mathbf{C}^0(\mathbf{x},\mathbf{p}) \mathbf{S}_{\mathbf{x}}^{0,1}(\mathbf{p},\mathbf{q})\, dV_{\mathbf{p}} \qquad \forall \mathbf{x}, \mathbf{q} \in \mathcal{B}^1. \tag{11}$$

Equation (10) involves quantities that are defined only in the level 1 body $\mathcal{B}^1$. Therefore, it provides a coarsened description of the internal forces in the level 0 body. The coarsened micromodulus function defined in (11) takes into account the equilibrium of points in $\mathcal{B}^0 - \mathcal{B}^1$ and their effect on the forces in $\mathcal{B}^1$.

Restricting the volume of integration in the above steps to a sphere of radius r^1 in effect assumes that the internal forces on any $\mathbf{x} \in \mathcal{B}^1$ can be obtained accurately while neglecting all interactions between the interior and exterior of the sphere centered at $\mathbf{x}$. The value of r^1 must be chosen large enough so that this is true. To find a suitable value, the procedure described above can be repeated with increasing choices of r^1. At some point in this process, the values of $\mathbf{C}^1(\mathbf{x},\mathbf{q})$ computed from (11) will become negligible for all $\mathbf{q}$ such that $|\mathbf{q}-\mathbf{x}| > r^1$. This implies that further increases to r^1 will have no effect on $\mathbf{C}^1$; therefore this value of r^1 is sufficiently large to satisfy the assumptions in the analysis.

Equations (2) and (9) assert that the displacements and the force densities agree between the level 0 and level 1 models on $\mathcal{B}^1$. This implies that the solution in $\mathcal{B}^1$ to any equilibrium boundary value problem, in which boundary data $\mathbf{b}$ or $\mathbf{u}$ are specified on part of $\mathcal{B}^1$, is independent of whether we use the level 0 or level 1 model. In this sense, the level 1 model exactly duplicates the level 0 model, but with fewer degrees of freedom.

3 Successive coarsening levels

Recall that the micromodulus function in the level 1 model given by (11) involve only points $\mathbf{x}$ and $\mathbf{q}$ in $\mathcal{B}^1$. So, the level 1 equilibrium problem has exactly the same mathematical structure as the original level 0 problem, but with quantities defined on $\mathcal{B}^1$ instead of $\mathcal{B}^0$. Therefore, the entire coarsening process can be repeated over and over in the same way, each time increasing the length scale.

Define $\mathcal{B}^M \subset \mathcal{B}^{M-1} \subset \cdots \subset \mathcal{B}^0$ (Figure 1). Each $\mathcal{B}^m$ is called the *level m body*. For any $\mathbf{x} \in \mathcal{B}^m$, let $\mathcal{N}_{\mathbf{x}}^m$ be the closed neighborhood in $\mathcal{B}^{m-1}$ with radius r^m, and let $\mathcal{R}_{\mathbf{x}}^m = \mathcal{N}_{\mathbf{x}}^m \cap \mathcal{B}^m$. Then, following the steps (2) through (11), for any $M \geq m \geq 1$,

$$\mathbf{u}^{m-1}(\mathbf{p}) = \mathbf{u}^m(\mathbf{p}) \qquad \forall \mathbf{p} \in \mathcal{R}_{\mathbf{x}}^m,$$

$$\mathbf{L}^{m-1}(\mathbf{z}) + \mathbf{b}(\mathbf{z}) = \mathbf{0} \qquad \forall \mathbf{z} \in \mathcal{N}_{\mathbf{x}}^m - \mathcal{R}_{\mathbf{x}}^m,$$

$$\mathbf{b}(\mathbf{z}) = \mathbf{0} \qquad \forall \mathbf{z} \in \mathcal{N}_{\mathbf{x}}^m - \mathcal{R}_{\mathbf{x}}^m.$$

For this choice of $\mathbf{x} \in \mathcal{B}^m$, evaluate the resolvent kernel $\mathbf{S}_{\mathbf{x}}^{m-1,m}$:

$$\mathbf{u}^{m-1}(\mathbf{p}) = \int_{\mathcal{R}_{\mathbf{x}}^m} \mathbf{S}_{\mathbf{x}}^{m-1,m}(\mathbf{p},\mathbf{q})\mathbf{u}^m(\mathbf{q})\, dV_{\mathbf{q}} \qquad \forall \mathbf{p} \in \mathcal{N}_{\mathbf{x}}^m. \tag{12}$$

The level m force density is then

$$\mathbf{L}^m(\mathbf{x}) = \int_{\mathcal{R}_{\mathbf{x}}^m} \mathbf{C}^m(\mathbf{x},\mathbf{q})(\mathbf{u}^m(\mathbf{q}) - \mathbf{u}^m(\mathbf{x}))\, dV_{\mathbf{q}} \qquad \forall \mathbf{x} \in \mathcal{B}^m$$

where $\mathbf{C}^m : \mathcal{B}^m \times \mathcal{B}^m$ is defined by

$$\mathbf{C}^m(\mathbf{x},\mathbf{q}) = \int_{\mathcal{N}_{\mathbf{x}}^m} \mathbf{C}^{m-1}(\mathbf{x},\mathbf{p})\mathbf{S}_{\mathbf{x}}^{m-1,m}(\mathbf{p},\mathbf{q})\, dV_{\mathbf{p}} \qquad \forall \mathbf{x},\mathbf{q} \in \mathcal{B}^m.$$

With each successive coarsening, more material is excluded, and the length scale is increased.

4 Discretized method

To carry out the coarsening numerically, the level 0 body $\mathcal{B}^0$ is discretized into nodes which, for simplicity, all have equal volume v. Each node i has position $\mathbf{x}_i$ and level m_i. For any nodes i and j, let

$$\mathbf{C}_{i,j}^0 = v\mathbf{C}^0(\mathbf{x}_i,\mathbf{x}_j).$$

To find the coarsened micromodulus for node i, it is first necessary to find the resolvent kernel defined by (6). A convenient way to do this numerically is

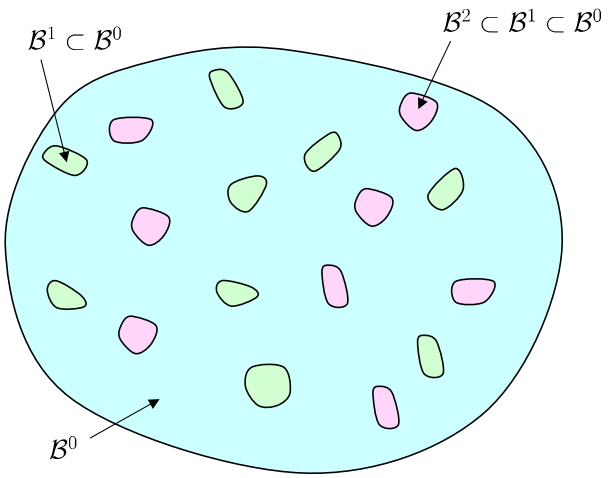

Figure 1: Levels 0, 1, and 2 in a peridynamic body.

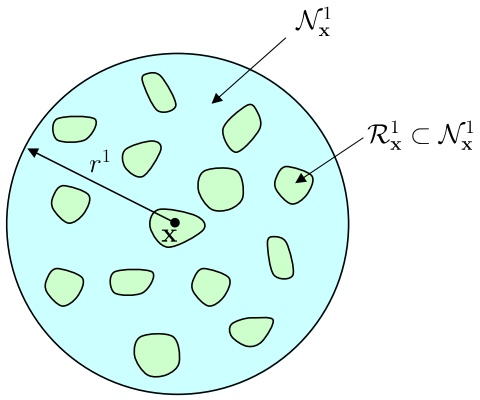

Figure 2: Neighborhood $\mathcal{N}_x^1$ with coarsened subset $\mathcal{R}_{\mathbf{x}}^1$.

to use a vector of unknowns $\{u^0\}$ in which the nodes within $\mathcal{R}_i^1$ are grouped at the top. The corresponding displacements are forced to coincide with the values of $\mathbf{u}^1$ according to the compatibility condition (2). This condition is enforced by placing 0's on the rows of the matrix for these degrees of freedom, with 1 on the diagonal. The remaining degrees of freedom, which correspond to nodes in $\mathcal{N}_i^1 - \mathcal{R}_i^1$, are determined by the equilibrium conditions (3), (4), and (5). The resulting matrix equation has the following form:

$$\begin{bmatrix} \mathbf{1} & 0 & 0 & 0 & \dots & & \\ \vdots & & & & & & \\ \dots & 0 & \mathbf{1} & 0 & 0\dots & & \\ \vdots & & & & & & \\ \dots & & \mathbf{C}^0_{i,i-1} & -\mathbf{P}_i & \mathbf{C}^0_{i,i+1} & & \dots \\ \vdots & & & & & & \\ & & & \dots & & \mathbf{C}^0_{N,N-1} & -\mathbf{P}^0_N \end{bmatrix} \begin{Bmatrix} \mathbf{u}_1^0 \\ \vdots \\ \mathbf{u}_R^0 \\ \vdots \\ \mathbf{u}_i^0 \\ \vdots \\ \mathbf{u}_N^0 \end{Bmatrix} = \begin{Bmatrix} \mathbf{u}_1^1 \\ \vdots \\ \mathbf{u}_R^1 \\ \vdots \\ \mathbf{0} \\ \vdots \\ \mathbf{0} \end{Bmatrix}$$

where R is the number of nodes in $\mathcal{R}_i^1$ and N is the number of nodes in $\mathcal{N}_i^1$. The diagonal matrix elements $\mathbf{P}_i$ are defined by

$$\mathbf{P}_i = \sum_{j \neq i} \mathbf{C}^0_{i,j}.$$

The above matrix equation will be abbreviated as

$$[A]\{u^0\} = \{b\}. \tag{13}$$

where $[A]$ is an $N \times N$ matrix. Let $[A]^{-1}$ be the inverse of this matrix, therefore

$$[A]^{-1}\{b\} = \{u^0\}.$$

Now define a $N \times R$ matrix $[S^{0,1}]$ to be the leftmost R columns of $[A]^{-1}$. Then

$$\{u^0\} = [S^{0,1}]\{u^1\} \tag{14}$$

where

$$\{u^1\} = \begin{Bmatrix} \mathbf{u}_1^1 \\ \vdots \\ \mathbf{u}_R^1 \end{Bmatrix}$$

Equation (14) provides the discretized representation of (6).

To evaluate the coarsened micromoduli $\mathbf{C}^1_{i,j}$, (11) is discretized as follows:

$$\mathbf{C}^1_{i,j} = v \sum_{k=1}^{N} \mathbf{C}^0_{i,k} \mathbf{S}^{0,1}_{k,j}$$

where the $\mathbf{S}_{k,j}^{0,1}$ are the elements of the matrix $[S^{0,1}]$ found above, each of which is a second order tensor.

Successive coarsenings to higher levels are done in the same way, thus, for any $m \geq 1$,

$$\mathbf{C}_{i,j}^{m} = v \sum_{k=1}^{N^m} \mathbf{C}_{i,k}^{m-1} \mathbf{S}_{k,j}^{m-1,m}$$

where the $[S^{m-1,m}]$ components are found by inverting the $[A]$ matrix

$$[A] = \begin{bmatrix} \mathbf{1} & 0 & 0 & 0 & \dots & & \\ \vdots & & & & & & \\ \dots & 0 & \mathbf{1} & 0 & 0 \dots & & \\ \vdots & & & & & & \\ \dots & & \mathbf{C}_{i,i-1}^{m-1} & -\mathbf{P}_{i}^{m-1} & \mathbf{C}_{i,i+1}^{m-1} & & \dots \\ \vdots & & & & & & \\ & & & \dots & & \mathbf{C}_{N,N-1}^{m-1} & -\mathbf{P}_{N}^{m-1} \end{bmatrix}.$$

Note that each new coarsening only uses quantities from the previous level.

5 Examples

These numerical example problems illustrate the general form of the coarsened micromodulus function (Example 1), the effect of a periodic microstructure (Example 2), and the properties of the method applied to a defect in an otherwise homogeneous body (Example 3). In all cases, the coarsened micromulus functions are evaluated for every discretized node i. Gaussian elimination is used to find the matrix inverse $[A]^{-1}$ as discussed in the previous section. The discretized boundary value problems are also solved using Gaussian elimination.

5.1 Micromodulus in a homogeneous bar

This example illustrates the typical form of coarsened micromodulus functions. A homogeneous, one dimensional bar of length 1.0 has a tent-shaped micromodulus function C^0 as shown in Figure 3:

$$C^0(x,q) = \begin{cases} 1 - |q-x|/r^0 & \text{if } 0 < |q-x| < r^0, \\ 0 & \text{otherwise.} \end{cases}$$

The level 0 interaction distance is $r^0 = 0.05$. The bar is discretized into nodes with spacing $v = 0.005$, thus $r^0 = 10v$.

Coarsening is carried out as shown schematically in Figure 4. Every fourth node in level 0 is also in level 1. Every second node in level 1 is also

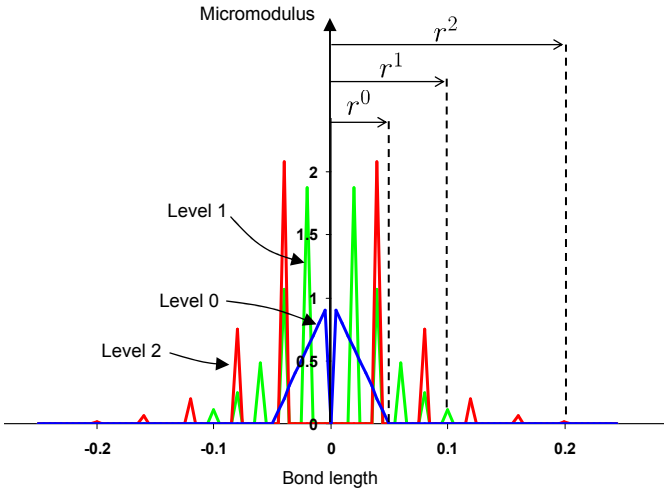

Figure 3: Micromodulus functions C^0, C^1, and C^2 in a homogeneous one-dimensional bar. The level 1 and 2 curves have peaks because they are not defined everywhere, only in the coarsened grids.

in level 2. The coarsened micromodulus functions C^1 and C^2 are shown as functions of bond distance $q - x$ in the figure. These curves have sharp peaks because they are defined only in their respective coarsened regions, *i.e.,* every fourth or eighth node in the grid.

5.2 Bar with periodic microstructure

This example illustrates the properties of the coarsening procedure when applied to a composite material. A bar with length 1.0 is composed of alternating stripes $\mathcal{S}_{\text{hard}}$ and $\mathcal{S}_{\text{soft}}$. (These represent the physical properties of the level 0 model and should not be confused with the coarsening levels.) Each stripe has width 0.05. The interaction distance r^0 is also 0.05. The micromodulus is given by

$$C^0(x,q) = \begin{cases} 10 & \text{if } 0 < |q-x| < r^0 \text{ and } (x \in \mathcal{S}_{\text{hard}} \text{ and } q \in \mathcal{S}_{\text{hard}}), \\ 1 & \text{if } 0 < |q-x| < r^0 \text{ and } (x \in \mathcal{S}_{\text{soft}} \text{ or } q \in \mathcal{S}_{\text{soft}}), \\ 0 & \text{otherwise.} \end{cases}$$

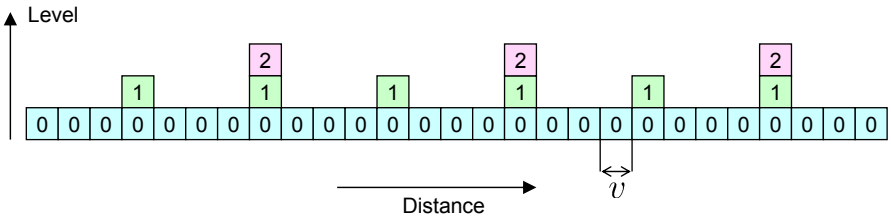

Figure 4: Coarsening levels 0, 1, and 2 for the one dimensional bar in Examples 1 and 2. Each box in the figure represents one node in the discretized model. Nodes in level m also belong to all levels lower than m.

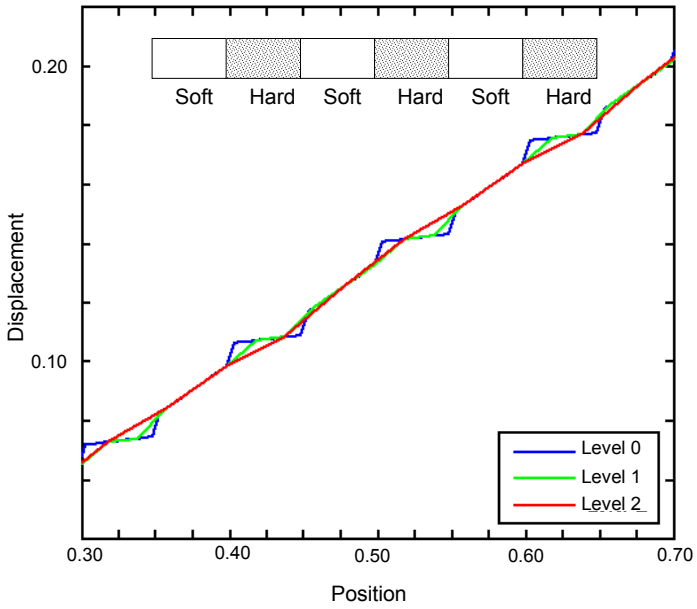

Figure 5: Displacement fields for coarsening levels 0, 1, and 2 within the composite material in Example 2.

In other words, bonds that have both ends in a hard stripe have hard properties. Bonds that have either end or both ends in a soft stripe have soft properties.

The level 0 interaction distance is $r^0 = 0.05$. The discretized model has a spacing of 0.005. The coarsened levels are the same as in the previous example and shown in Figure 4.

The boundary conditions are as follows. The leftmost three level 2 nodes are constrained to have zero displacement. The rightmost three level 2 nodes have an applied body force density of $b = 0.001$. The computed displacements with the identical boudary conditions for coarsening levels 0, 1, and 2 are shown in Figure 5. As expected, the level 0 solution contains the greatest level of detail due to the microstructure. Levels 1 and 2 smooth out these features. However, both coarsened levels have the same global stretch as the detailed solution. This demonstrates that the effective properties produced by the coarsening method accurately reflect the bulk properties of the composite.

5.3 Homogeneous bar with a defect

This example illustrates the response of a coarsened model when the level 0 body contains a small defect. The material model is the same as in Example 1, but with a term μ that degrades the stiffness of bonds that cross the location of a defect x_d:

$$C^0(x,q) = \mu(x,q) \begin{cases} 1 - |q-x|/r^0 & \text{if } 0 < |q-x| < r^0, \\ 0 & \text{otherwise.} \end{cases}$$

where

$$\mu(x,q) = \begin{cases} 0.1 & \text{if } x \le x_d \le q \text{ or } q \le x_d \le x \\ 1 & \text{otherwise.} \end{cases}$$

The level 0 interaction distance is $r^0 = 0.05$. The bar is discretized into nodes with spacing $v = 0.005$, thus $r^0 = 10v$. The defect is located at the center of the bar.

The level 1 grid contains every third node of the level 0 grid. The level 2 grid contains every third node of the level 1 grid (Figure 6). Prescribed displacement boundary conditions are applied to three leftmost level 2 nodes and to the three rightmost level 2 nodes. The values of the prescribed displacements at these nodes are given by $u_i^0 = u_i^1 = u_i^2 = x_i$ where x_i is the position of the node.

The resulting fields u^0, u^1, and u^2 near the defect are shown in Figure 7. The three levels give nearly identical results except that the jump in displacement across the defect reflects the wider spacing between nodes in the coarsened grids.

6 Computational cost

To determine the implications of coarsening for the computational effort in a numerical model, consider the effect of increasing the total volume of the level 0 body. Assuming the discretization spacing and level 0 material model are constant, let the total number of level 0 nodes in the model be K_0, which is proportional to the total volume of material. Suppose the linear solver, which is applied to the fully coarsened level M grid, uses $J = aK_M^n$ arithmetic operations, where a and n are constants, and K_M is the total number of nodes in level M. (For Gaussian elimination, $n = 3$, although more efficient methods are available.) Suppose each the grid for each level has $1/L$ as many nodes as in the previous level, where L is a constant. (In Example 3, $L = 3$. If this example were three dimensional, then we would have $L = 3^3$.) So, $K_M = K_0/L^M$.

The computational effort in determining the level $m+1$ properties from the level m properties is proportional to K_m, since the inverse matrix $[A]^{-1}$

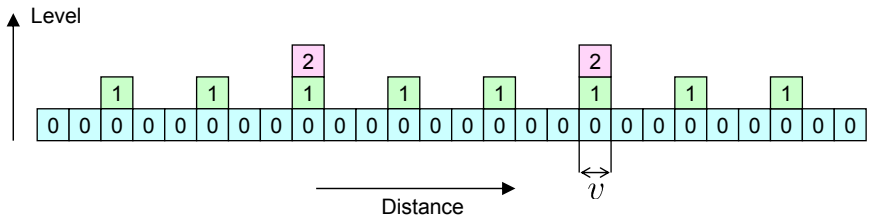

Figure 6: Coarsening levels 0, 1, and 2 for the one dimensional bar in Example 3.

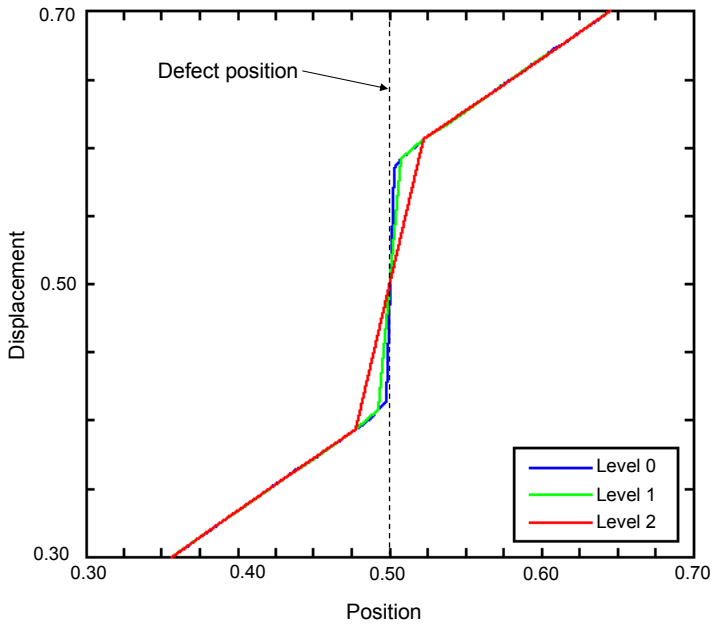

Figure 7: Coarsened displacement fields in a bar with a defect, Example 3.

must be computed for each level m node. Therefore, we can write, for some positive constant b,

$$\begin{aligned} J &= a\left(\frac{K_0}{L^M}\right)^n + \sum_{m=0}^{M-1} \frac{bK_0}{L^m} \\ &= a\left(\frac{K_0}{L^M}\right)^n + bK_0 \frac{1-1/L^M}{1-1/L} \\ &< a\left(\frac{K_0}{L^M}\right)^n + bK_0 \frac{L}{L-1}. \end{aligned}$$

The conclusion is that by coarsening up to level M, the computational effort in the linear solve for a boundary value problem is reduced by a factor of L^{nM} over what it would be if the whole problem were solved in level 0. In a three dimensional version of Example 3, with Gaussian elimination, this factor would be 81^M. The price paid in determining the coarsened properties is a computational effort of less than $bK_0L/(L-1)$, independent of M.

7 Discussion

The coarsening method described above involves an increase in the length scale r^m at each step in the process. In this sense, it provides a tool for multiscale analysis. Although it involves derivation of material properties at variable length scales, the method is different from *rescaling* of material properties as discussed in [3, 8]. In these references, the technique for changing length scales starts with a small-scale material model and maps each bond explicitly into a rescaled bond strictly according to bond length. Such a rescaling approach would not be expected to accurately reproduce the effective properties of a heterogeneous material, such as a composite, because it does not account for the rearrangement of material at the small scale in response to deformation at the large scale. The present approach to coarsening does account for this rearrangement, as demonstrated in Example 2.

The development in this paper treats only the linearized, equilibrium case. However, the coarsened material properties developed here are expected to be useful in dynamic problems as well. Future work will investigate the implications for the *time* scale of the material when the length scale is increased from r^0 to r^m. It is expected that there is a strong connection between length and time scales in the peridynamic model because the length scale dictates the highest vibrational frequencies that can be sustained by the continuum. Future work will also attempt to treat nonlinearities in the coarsening method through an incremental approach in which the linearized material properties $\mathbf{C}^0$ are re-evaluated as the problem evolves.

The coarsening method proposed here is similar in some ways to a method investigated by Eom [7] for coarse-graining an elastic network model of a protein molecule [12]. In Eom's coarse graining approach, atoms in a macromolecular structure are designated as master and slave atoms, the latter of which are in equilibrium but coupled to the former.

Since a system of discrete particles can be represented exactly as a peridynamic body [8], it is plausible that the method presented here could be applied to atomic systems, resulting in a coarse-graining of atomistics. Such an application would require the thermal motion of particles to be incorporated into the detailed material properties $\mathbf{C}^0$. Molecular dynamics simulation may provide a means to accomplish this by providing time averages of forces between atoms.

Acknowledgments

The author gratefully acknowledges helpful discussions with Drs. John Aidun, Abe Askari, Florin Bobaru, Richard B. Lehoucq, Michael L. Parks, and Olaf Weckner. This work was performed under a Laboratory Directed Research and Development project at Sandia National Laboratories. Sandia is a multiprogram laboratory operated by Sandia Corporation, a Lockheed Martin Company, for the United States Department of Energy's National Nuclear Security Administration under contract DE-AC04-94AL85000.

References

[1] B. Alali and R. Lipton. Multiscale analysis of heterogeneous media in the peridynamic formulation. Technical Report IMA Preprint Series 2241, Institute for Mathematics and Its Applications, Minneapolis, Minnesota, USA, 2009.

[2] E. Askari, F. Bobaru, R. B. Lehoucq, M. L. Parks, S. A. Silling, and O. Weckner. Peridynamics for multiscale materials modeling. *Journal of Physics: Conference Series*, 125(012078), 2008.

[3] F. Bobaru, M. Yang, L. F. Alves, S. A. Silling, A. Askari, and J. Xu. Convergence, adaptive refinement, and scaling in 1d peridynamics. *International Journal for Numerical Methods in Engineering*, 77:852–877, 2008.

[4] E. Emmrich and O. Weckner. Analysis and numerical approximation of an integrodifferential equation modeling non-local effects in linear elasticity. *Mathematics and Mechanics of Solids*, 12:363–384, 2005.

[5] E. Emmrich and O. Weckner. On the well-posedness of the linear peridynamic model and its convergence towards the Navier equation of linear elasticity. *Communications in Mathematical Sciences*, 5:851–864, 2007.

[6] E. Emmrich and O. Weckner. The peridynamic equation and its spatial discretization. *Mathematical Modelling and Analysis*, 12, 2007.

[7] K. Eom, S.-C. Baek, J.-H. Ahn, and S. Na. Coarse-graining of protein structures for the normal mode studies. *Journal of Computational Chemistry*, 28:1400–1410, 2007.

[8] R. B. Lehoucq and S. A. Silling. Statistical coarse-graining of molecular dynamics into peridynamics. Technical Report SAND2007-6410, Sandia National Laboratories, Albuquerque, New Mexico 87185 and Livermore, California 94550, October 2007.

[9] S. A. Silling. Linearized theory of peridynamic states. *Journal of Elasticity*, 99:85–111, 2010.

[10] S. A. Silling, M. Epton, O. Weckner, J. Xu, and E. Askari. Peridynamic states and constitutive modeling. *J. Elasticity*, 88:151–184, 2007.

[11] S. A. Silling, M. Zimmermann, and R. Abeyaratne. Deformation of a peridynamic bar. *J. Elasticity*, 73:173–190, 2003.

[12] M. M. Tirion. Large amplitude elastic motions in proteins from a single-parameter, atomic analysis. *Physical Review Letters*, 77:1905–1908, 1996.

[13] O. Weckner and R. Abeyaratne. The effect of long-range forces on the dynamics of a bar. *Journal of the Mechanics and Physics of Solids*, 53:705–728, 2005.

[14] O. Weckner, G. Brunk, M. A. Epton, S. A. Silling, and E. Askari. Green's functions in non-local three-dimensional linear elasticity. *Proceedings of the Royal Society A*, 465:3463–3487, 2009.

[15] O. Weckner and E. Emmrich. Numerical simulation of the dynamics of a nonlocal, inhomogeneous, infinite bar. *Journal of Computational and Applied Mechanics*, 6:311–319, 2005.